Quantum transitions of the isotropic *XY* model with long-range interactions on the inhomogeneous periodic chain

J. P. de Lima
Departamento de Física, Universidade Federal do Piauí, Campus Ministro Petrônio Portela, Teresina, Piauí 64049-550, Brazil

L. L. Gonçalves*
Departamento de Engenharia Metalúrgica e de Materiais, Universidade Federal do Ceará, Campus do Pici, Bloco 714, Fortaleza, Ceará 60455-760, Brazil

(Received 10 March 2008; revised manuscript received 2 May 2008; published 18 June 2008)

The isotropic *XY* model ($s=1/2$) in a transverse field, with uniform long-range interactions among the transverse components of the spins, on the inhomogeneous periodic chain, is studied. The model, composed of *N* segments with *n* different exchange interactions and magnetic moments, is exactly solved by introducing the integral Gaussian transformation and the generalized Jordan–Wigner transformation, which reduce the problem to the diagonalization of a finite matrix of *n*th order. The quantum transitions induced by the transverse field are determined by analyzing the induced magnetization of the cell and the equation of state. The phase diagrams for the quantum transitions, in the space generated by the transverse field and the interaction parameters, are presented. As expected, the model presents multiple, first- and second-order quantum transitions induced by the transverse field, and it corresponds to an extension of the models recently considered by the authors. Detailed results are also presented, at $T=0$, for the induced magnetization and isothermal susceptibility χ_T^{zz} as a function of the transverse field.

DOI: 10.1103/PhysRevB.77.214424 PACS number(s): 75.10.Jm, 05.70.Fh, 05.70.Jk, 75.10.Pq

I. INTRODUCTION

The study of the critical quantum behavior of systems,[1] which is induced by quantum fluctuations, has been object of great interest in recent years. This critical behavior, which controls the properties of the systems at very low temperature, is present in different systems. In particular, for magnetic systems, they have been responsible for unusual properties observed in low dimensional magnetic materials.[2,3] Therefore, the study of the critical behavior of spin systems in low dimension, particularly the exactly soluble, is of great importance for understanding the properties of these materials.

Among these models, the one-dimensional *XY* model introduced by Lieb *et al.*,[4] despite being almost 50 years old, is still the best one to describe exactly magnetic quantum transitions. The rather rich quantum critical behavior presented by the model can be seen in a recent work by de Lima *et al.*[5] and in the references therein, where they studied the anisotropic model on the inhomogeneous periodic lattice. The study of the model on the inhomogeneous open lattice has also been recently addressed by Feldman.[6]

The isotropic model on the inhomogeneous lattice has also been studied by de Lima *et al.*,[7] where a detailed study of the static and dynamic critical properties is presented. Although the model has been applied mostly in the study of the quantum critical behavior of magnetic systems,[2,3,8–10] more recently it has also been applied in the study of quantum entanglement, which plays an essential role in the quantum computation. These applications can be found in the recent work by Amico *et al.*[11] and in the references therein. In particular, in a recent work on quantum communication in a spin system, Avellino *et al.*[12] studied the strong effect of long-range interaction on the fidelity of transmission of quantum information. Besides the importance of the long-range interaction in the transmission of quantum information in spin chains, its presence can induce classical critical behavior in these systems, which is essential for the study of the classical and/or quantum crossover.

The one-dimensional *XY* model is among the models which present this behavior, provided a uniform long-range interaction is considered. In particular, for the isotropic one, in the presence of a homogeneous long-range interaction along the transverse field direction, it can still be solved exactly, and its solution has been obtained by Gonçalves *et al.*[13,14] Besides the appearance of classical critical behavior, the most important features presented by the homogeneous model have been the existence of quantum bicritical points and, particularly, the existence of first-order quantum transitions. Another relevant results obtained in the study of the homogeneous case were the exact determination of the classical and/or quantum crossover for first- and second-order phase transitions and the verification of the scaling relations proposed by Continentino and Ferreira[15] for first-order quantum transitions.

As pointed out by Pfleiderer,[16] quantum first-order transitions can be driven by different mechanisms, and to look at this quantum critical behavior, in an exactly soluble problem, has been the one of the motivations to analyze the isotropic model on the inhomogeneous periodic chain with long-range interaction. Besides this point, the possibility of having multiple first- and second-order quantum transitions and multicritical points of higher order has also been important motivation for considering the long-range interaction in the inhomogeneous model.

Therefore, in this paper, we will extend our previous results[7,13,14] by looking at an extended version of the models previously considered. Although the model presents classical

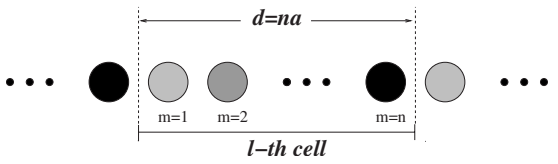

FIG. 1. Unit cell of the inhomogeneous chain.

and quantum critical behaviors, we will restrict our analysis to the quantum one.

In Sec. II we present the exact solution of the model and obtain the functional of the Helmholtz free energy at arbitrary temperatures. The quantum critical behavior is discussed in Sec. III, and it is determined from the equation of state at $T=0$. Explicit results for the quantum phase diagrams, induced magnetization M^z, and isothermal susceptibility χ_T^{zz} for systems with different sizes of the unit cell are also presented. Finally in Sec. IV we summarize the main results of the paper.

II. MODEL AND FUNCTIONAL OF THE FREE ENERGY

We consider the isotropic XY model ($s=1/2$) on the inhomogeneous periodic chain with N cells, n sites per cell, and lattice parameter a, in a transverse field, with long-range interactions among the spin components in the z direction. The unit cell of the inhomogeneous lattice is shown in Fig. 1, and the Hamiltonian of the model in its more general form is given by

$$H = -\sum_{l=1}^{N}\{\sum_{m=1}^{n}\mu_m h S_{l,m}^z \sum_{m=1}^{n-1} J_m[S_{l,m}^x S_{l,m+1}^x + S_{l,m}^y S_{l,m+1}^y] + J_n S_{l,n}^x S_{l+1,1}^x + J_n S_{l,n}^y S_{l+1,1}^y\} - \frac{J'}{N}\sum_{j=1}^{N}\sum_{l=1}^{N}\sum_{m,m'=1}^{n} S_{j,m}^z S_{l,m'}^z, \tag{1}$$

where the parameters J_m are the exchange coupling between nearest neighbors, μ_m the magnetic moments, h the external field, and J' the uniform long-range interaction among the z components, and where we have assumed periodic boundary conditions. If we introduce the ladder operators,

$$S^{\pm} = S^x \pm iS^y, \tag{2}$$

and the Jordan–Wigner transformations,

$$S_{l,m}^{+} = \exp\, i\pi\sum_{l'=1}^{l-1}\{\sum_{m'=1}^{n} c_{l',m'}^{\dagger}c_{l',m'} + i\pi\sum_{m'=1}^{m-1} c_{l,m'}^{\dagger}c_{l,m'}\}c_{l,m}^{\dagger}, \tag{3}$$

$$S_{l,m}^{z} = c_{l,m}^{\dagger}c_{l,m} - \frac{1}{2}, \tag{4}$$

where $c_{l,m}$ and $c_{l,m}^{\dagger}$ are fermion annihilation and creation operators, we can write the Hamiltonian as[17]

$$H = H^{+}P^{+} + H^{-}P^{-}, \tag{5}$$

where

$$H^{\pm} = -\sum_{l=1}^{N}\left\{\sum_{m=1}^{n}\left[(\mu_m h - J')c_{l,m}^{\dagger}c_{l,m} - \frac{1}{2}\left(\mu_m h - \frac{J'}{2}\right)\right] + \sum_{m=1}^{n-1}\frac{J_m}{2}(c_{l,m}^{\dagger}c_{l,m+1} + c_{l,m+1}^{\dagger}c_{l,m})\right\} - \sum_{l=1}^{N-1}\frac{J_n}{2}(c_{l,n}^{\dagger}c_{l+1,1} + c_{l+1,1}^{\dagger}c_{l,n}) \pm \frac{J_n}{2}(c_{N,n}^{\dagger}c_{1,1} + c_{1,1}^{\dagger}c_{N,n}) - \frac{J'}{N}\sum_{j=1}^{N}\sum_{l=1}^{N}\sum_{m,m'=1}^{n} c_{j,m}^{\dagger}c_{j,m}c_{l,m'}^{\dagger}c_{l,m'} \tag{6}$$

and

$$P^{\pm} = \frac{I \pm P}{2}, \tag{7}$$

with P given by

$$P = \exp\left(i\pi\sum_{l=1}^{N}\sum_{m=1}^{n} c_{l,m}^{\dagger}c_{l,m}\right). \tag{8}$$

As it is well known,[17–19] since the operator P commutes with the Hamiltonian, the eigenstates have definite parity, and $P^{-}(P^{+})$ corresponds to a projector into a state of odd (even) parity. Introducing periodic and antiperiodic boundary conditions on c's for H^{-} and H^{+}, respectively, the wave vectors in the Fourier transforms,

$$c_{l,m} = \frac{1}{\sqrt{N}}\sum_{q}\exp(-iqdl)A_{q,m} \tag{9}$$

and

$$A_{q,m} = \frac{1}{\sqrt{N}}\sum_{l=1}^{N}\exp(iqdl)c_{l,m}, \tag{10}$$

are given by $q^{-}=\frac{2l\pi}{Nd}$ for periodic condition and $q^{+}=\frac{\pi(2l+1)}{Nd}$ for antiperiodic condition,[20] with $l=0,\pm 1,\ldots,\pm N/2$, and H^{-} and H^{+} can be written in the form

$$H^{\pm} = \sum_{q^{\pm}} H_{q^{\pm}}, \tag{11}$$

where

$$H_{q^{\pm}} = -\sum_{m=1}^{n}\left[(\mu_m h - J')A_{q^{\pm},m}^{\dagger}A_{q^{\pm},m} - \frac{1}{2}\left(\mu_m h - \frac{J'}{2}\right)\right] - \sum_{m=1}^{n-1}\frac{J_m}{2}[A_{q^{\pm},m}^{\dagger}A_{q^{\pm},m+1} + A_{q^{\pm},m+1}^{\dagger}A_{q^{\pm},m}] - \frac{J_n}{2}[A_{q^{\pm},n}^{\dagger}A_{q^{\pm},1}\exp(-idq^{\pm}) + A_{q^{\pm},1}^{\dagger}A_{q^{\pm},n}\exp(idq^{\pm})] - \frac{J'}{N}\sum_{m=1}^{n}(A_{q^{\pm},m}^{\dagger}A_{q^{\pm},m})^2. \tag{12}$$

Although H^{-} and H^{+} do not commute, it can be shown that in the thermodynamic limit, all the static properties of the sys-

tem can be obtained in terms of H^- or H^+.[17–19] Therefore, by considering periodic boundary conditions on c's, we can identify $H \equiv H^-$ and $q \equiv q^-$, where H_q can be written in the form

$$H_q = -\sum_{m=1}^{n}\left[(\mu_m h - J')A_{q,m}^{\dagger}A_{q,m} - \frac{1}{2}\left(\mu_m h - \frac{J'}{2}\right)\right] - \sum_{m=1}^{n-1}\frac{J_m}{2}[A_{q,m}^{\dagger}A_{q,m+1} + A_{q,m+1}^{\dagger}A_{q,m}] - \frac{J_n}{2}[A_{q,n}^{\dagger}A_{q,1}\exp(-idq) + A_{q,1}^{\dagger}A_{q,n}\exp(idq)] - \frac{J'}{N}\left(\sum_{m=1}^{n}A_{q,m}^{\dagger}A_{q,m}\right)^2. \quad (13)$$

The partition function is then given by

$$Z_N = \sqrt{\frac{N}{2\pi}}\prod_q (Z_q), \quad (14)$$

with

$$Z_q = \exp\left[-\frac{\beta}{2}\sum_{m=1}^{n}\left(\mu_m h - \frac{J'}{2}\right)\right] \times \exp\left\{\sum_{m=1}^{n-1}\frac{\beta J_m}{2}[A_{q,m}^{\dagger}A_{q,m+1} + A_{q,m+1}^{\dagger}A_{q,m}] + \frac{\beta J_n}{2}[A_{q,n}^{\dagger}A_{q,1}\exp(-idq) + A_{q,1}^{\dagger}A_{q,n}\exp(idq)] + \sum_{m=1}^{n}\beta(\mu_m h - J')A_{q,m}^{\dagger}A_{q,m} + \left(\sqrt{\frac{\beta J'}{N}}\sum_{m=1}^{n}A_{q,m}^{\dagger}A_{q,m}\right)^2\right\}. \quad (15)$$

Since the long-range interaction term commutes with the Hamiltonian, we can introduce the Gaussian transformation

$$\exp(b^2) = \frac{1}{\sqrt{2\pi}}\int_{-\infty}^{\infty}\exp\left(-\frac{x^2}{2} + \sqrt{2}bx\right)dx \quad (16)$$

in the previous expression, so that the partition function can be rewritten in an integral representation as

$$Z_q = \exp\left[-\frac{\beta}{2}\sum_{m=1}^{n}\left(\mu_m h - \frac{J'}{2}\right)\right]\int_{-\infty}^{\infty}\left[\exp\left(-\frac{\bar{x}^2}{2}\right)\right] \times \mathrm{Tr}[\exp(-\beta\widetilde{H_q}(\bar{x}))],$$

where $\bar{x} = x/\sqrt{nN}$ and the effective Hamiltonian $\widetilde{H_q}(\bar{x})$ is given by

$$\widetilde{H}_q(\bar{x}) = -\sum_{m=1}^{n-1}\frac{J_m}{2}[A_{q,m}^{\dagger}A_{q,m+1} + A_{q,m+1}^{\dagger}A_{q,m}] - \frac{J_n}{2}[A_{q,n}^{\dagger}A_{q,1}\exp(-idq) + A_{q,1}^{\dagger}A_{q,n}\exp(idq)] - \sum_{m=1}^{n}\left(\mu_m h - J' + \sqrt{\frac{2J'}{\beta}}\bar{x}\right)A_{q,m}^{\dagger}A_{q,m}. \quad (17)$$

By introducing the canonical transformations

$$A_{q,m} = \sum_{k=1}^{n}u_{q,km}\xi_{q,k}, \quad A_{q,m}^{\dagger} = \sum_{k=1}^{n}u_{q,km}^{*}\xi_{q,k}^{\dagger} \quad (18)$$

and by imposing the condition

$$[\xi_{q,k}, \widetilde{H}_q(\bar{x})] = \varepsilon_{q,k}\xi_{q,k}, \quad (19)$$

this leads, for the coefficients $u_{q,km}$, to the equation

$$\mathbf{A}_q\begin{pmatrix}u_{q,k1}\\ u_{q,k2}\\ \vdots\\ u_{q,kn}\end{pmatrix} = \varepsilon_{q,k}\begin{pmatrix}u_{q,k1}\\ u_{q,k2}\\ \vdots\\ u_{q,kn}\end{pmatrix}, \quad (20)$$

where $\mathbf{A}_q$ is given by

$$\mathbf{A}_q \equiv -\begin{pmatrix} \tilde{h}_1 & \frac{J_1}{2} & 0 & \cdots & 0 & \frac{J_n}{2}\exp(-iqd) \\ \frac{J_1}{2} & \tilde{h}_2 & \frac{J_2}{2} & & & 0 \\ 0 & \frac{J_2}{2} & \tilde{h}_3 & \frac{J_3}{2} & & \vdots \\ \vdots & & \frac{J_3}{2} & \ddots & \ddots & 0 \\ 0 & & & \ddots & \tilde{h}_{n-1} & \frac{J_{n-1}}{2} \\ \frac{J_n}{2}\exp(iqd) & 0 & \cdots & 0 & \frac{J_{n-1}}{2} & \tilde{h}_n \end{pmatrix}, \quad (21)$$

and the u's satisfy the orthogonality relations,

$$\sum_{m=1}^{n}u_{q,km}u_{q,k'm}^{*} = \delta_{kk'}, \quad (22)$$

$$\sum_{k=1}^{n}u_{q,km}u_{q,km'}^{*} = \delta_{mm'}, \quad (23)$$

and $\tilde{h}_j = \mu_m h - J' + \sqrt{\frac{2J'}{\beta}}\bar{x}$. Therefore, the effective Hamiltonian can be written in the diagonal form,

$$\widetilde{H}_q(\bar{x}) = \sum_k \tilde{\varepsilon}_{q,k}\eta_{q,k}^{\dagger}\eta_{q,k}, \quad (24)$$

where the spectrum $\tilde{\varepsilon}_q$ of H_q is determined from the determinant equation

$$\det(\mathbf{A}_q - \tilde{\varepsilon}_q \mathbf{I}) = 0, \tag{25}$$

and the operators η's are given in terms of A's and c's by the expression

$$\eta_{q,k} = \sum_{m=1}^{n} u^*_{q,km} A_{q,m} = \frac{1}{\sqrt{N}} \sum_{l=1}^{N} \sum_{m=1}^{n} \exp(iqdl) u^*_{q,km} c_{l,m}, \tag{26}$$

which have been obtained by using Eqs. (9) and (22). From this result, the partition function can be written in the form

$$\exp\{\sum_{q,k} \ln[1 + \exp(-\beta \tilde{\varepsilon}_{q,k})]\} d\bar{x}. \tag{27}$$

In the thermodynamic limit, the partition function can be evaluated by Laplace method by imposing the condition that $g'(\bar{x}_0)=0$, where $g(\bar{x})$ is given by

$$g(\bar{x}) = -\frac{\bar{x}^2}{2} + \frac{1}{nN} \sum_{q,k} \{\ln[1 + \exp(-\beta \tilde{\varepsilon}_{q,k})]\},$$

and $\bar{x}_0$ is equal to

$$\bar{x}_0 = \frac{1}{nN} \sum_{q,k} \frac{\sqrt{2\beta J'}}{1 + \exp(-\beta \tilde{\varepsilon}_{q,k})},$$

which can be written in terms of the average induced magnetization M^z, defined as

$$M^z = \frac{1}{nN} \sum_{l,m} \mu_m \langle S^z_{l,m} \rangle = \frac{1}{nN} \sum_{q,k,m} \mu_m u^*_{q,km} u_{q,km} \langle \eta^\dagger_{q,k} \eta_{q,k} \rangle - \frac{1}{2}, \tag{28}$$

in the form

$$\frac{\bar{x}_0}{\sqrt{2\beta J'}} = M^z + \frac{1}{2}.$$

Finally, we can obtain from the previous results the functional of the Helmholtz free energy per lattice site which is given by

$$f = \frac{h}{2} - \frac{k_B T}{nN} \sum_{q,k} \ln[1 + \exp(-\beta \tilde{\varepsilon}_{q,k})] + J' M^z (M^z + 1). \tag{29}$$

The equation of state is obtained numerically from this functional by imposing the conditions

$$\frac{\partial f}{\partial M^z} = 0, \quad \frac{\partial^2 f}{\partial M^{z2}} > 0. \tag{30}$$

The numerical solution is more easily obtained for $n \leq 4$, where there are analytical solutions for Eqs. (20) and (25) (Ref. 7) and in the cases where we have uniform magnetic moments, namely, $\mu_m \equiv \mu$. In this situation, the term $-\Sigma^n_{l,m} \mu h S^z_{l,m}$ commutes with the Hamiltonian, and consequently the effect of the field is to shift the spectrum. This means that the solution of Eq. (25) can be written as

$$\tilde{\varepsilon}_{q,k} = \tilde{\varepsilon}^0_{q,k} - \mu h + J' - \sqrt{\frac{2J'}{\beta}} x_0 = \tilde{\varepsilon}^0_{q,k} - \mu h - 2J' M^z, \tag{31}$$

where $\tilde{\varepsilon}^0_{q,k}$ is the energy of the excitations of the model for zero transverse field and long-range interaction, and we identify the expression $\mu h + 2J' M^z$ as an effective field h_{eff}.[14]

III. QUANTUM CRITICAL BEHAVIOR

In the limit $T \to 0$, the functional of the Helmholtz free energy per lattice site [Eq. (29)] can be explicitly written as

$$f = \frac{F_N}{N} = \frac{h}{2} + J' M^z (M^z + 1) - \frac{1}{\pi n} \sum_{k=1}^{n} \int_0^{\bar{q}_k} \varepsilon_{q,k} dq_k, \tag{32}$$

where $\bar{q}_k$ is obtained by imposing the condition $\tilde{\varepsilon}_{q,k}=0$ and we have considered the lattice spacing $a=1$ and uniform magnetic moments $\mu=1$. Under these conditions the average induced magnetization M^z, given in Eq. (28), can also be written in the form

$$M^z = \frac{1}{2\pi n} \sum_{k=1}^{n} \int_0^{\bar{q}_k} \text{sgn}(\varepsilon_{q,k}) dq_k. \tag{33}$$

The quantum phase diagram is determined from the equation of state, which is obtained numerically from the previous equations by considering the conditions shown in Eq. (30), and in particular we can determine the magnetization as a function of the transverse field. As it is well known, the second-order phase transitions are determined by imposing the limit $M^z \to 0$ and it can be shown numerically, for arbitrary unit-cell sizes, that the critical field varies linearly with the long-range range interaction J' and that these phase transitions, as in the homogenous model,[14] occur for $J' < 0$ only.

The first-order phase transitions are determined by imposing the additional condition

$$f(M^z) = f(M^z_p), \tag{34}$$

where M^z_p are the magnetization plateaus, which are identical to the ones in the model without the long-range interaction.[7] This is due to the fact that, for uniform magnetic moments, the long-range interaction does preserve the azimutal symmetry of the model and consequently the magnetization plateaus satisfy the quantization condition[21]

$$n\left(\frac{\mu}{2} - M^z_p\right) = \mu \times \text{integer}, \tag{35}$$

which does only depend on the symmetry of the Hamiltonian.

As in the homogenous case,[14] the first-order phase transitions occur for $J' > 0$ only, and in this case, besides the bicritical points where the second-order lines meet the first-order ones,[13] there are triple points which correspond to the point where three first-order lines meet. From the magnetization as a function of the field, we can obtain the isothermal susceptibility χ^{zz}_T, which is given by

$$\chi^{zz}_T \equiv \frac{1}{n} \frac{\partial M^z}{\partial h}. \tag{36}$$

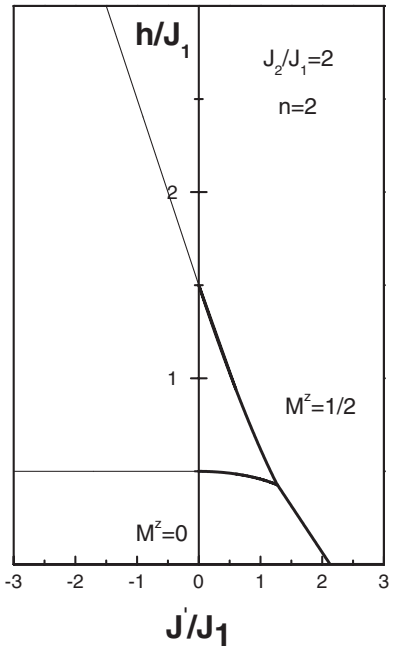

FIG. 2. Phase diagram for the quantum transitions as a function of the strength of the long-range interaction J'/J_1 for $n=2$ and $J_1=1$, $J_2=2$. For $J'/J_1>0$, the critical lines identify the first-order phase transitions and for $J'/J_1\leq 0$, the second-order phase transitions.

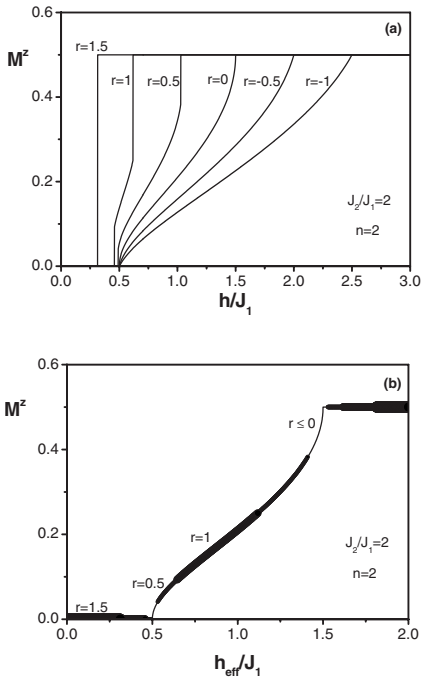

FIG. 3. (a) Magnetization as a function of h/J_1, and (b) universal curve for the magnetization as a function of the effective field h_{eff}/J_1 ($h_{\text{eff}}=h+2J'M^z$), at $T=0$, for different values of $r(r=J'/J_1)$, in the regions where the system undergoes first- ($r>0$) and second-order ($r\leq 0$) quantum transitions for $n=2$ and $J_1=1$, $J_2=2$.

The main results are shown in Figs. 2–11. In Fig. 2 we present the phase diagram for $n=2$, and as expected there are two second-order lines for $J'<0$ which end up at bicritical points for $J'=0$. For $J'>0$, there are two first-order lines which collapse into a single one at a triple point. In Fig. 3(a) we present the magnetization as a function of the field, and as it can be seen the different critical behaviors are explicitly shown depending on the sign of the long-range interaction. It should be noted that as we approach the triple point, the two first-order phase transitions collapse into a single one, which corresponds in this case to a jump in the induced magnetization from zero to one-half.

As in the homogeneous model,[14] there is a universal curve to which all magnetization data collapse, independently of the order of the transition. This is presented in Fig. 3(b), where we show the magnetization as a function of the effective field $h_{\text{eff}}=h+2J'M^z$.

In Fig. 4 we present the quantum phase diagram for $n=3$. As in the previous case, for $J'<0$ we have second-order phase transitions and for $J'>0$ we have first-order phase transitions. There are three second-order lines and two first-order lines meet at a unique triple point. The magnetization is presented in Fig. 5(a) for different values of J', which characterize the different behaviors, and in Fig. 5(b) we present the collapse of the magnetization when plotted as a function of the effective field h_{eff}.

It should be noted that for a different set of parameters, we could have two triple points, and in this case we will have a single first-order line beyond the critical value J', which is associated to the second triple point. This situation can be seen in the phase diagram shown in Fig. 6, for $n=4$, where it is explicitly shown that we can have three triple points. Since we have no suppression of a phase transition, there are four second-order transition lines. As it has been shown for $J'=0$,[7] an adequate choice of the exchange parameters can sup-

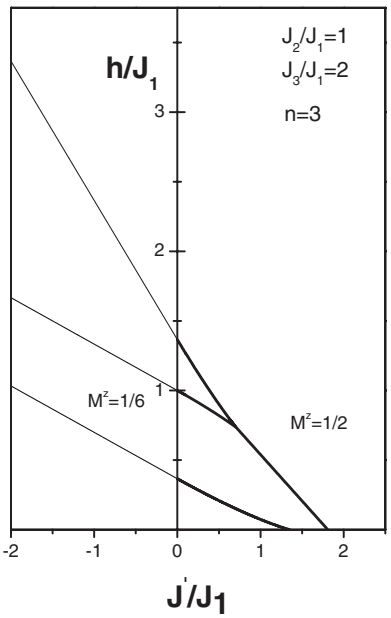

FIG. 4. Phase diagram for the quantum transitions as a function of the strength of the long-range interaction J'/J_1 for $n=3$ and $J_1=1$, $J_2=1$, and $J_3=2$. For $J'/J_1>0$, the critical lines identify the first-order phase transitions and for $J'/J_1\leq 0$, the second-order phase transitions.

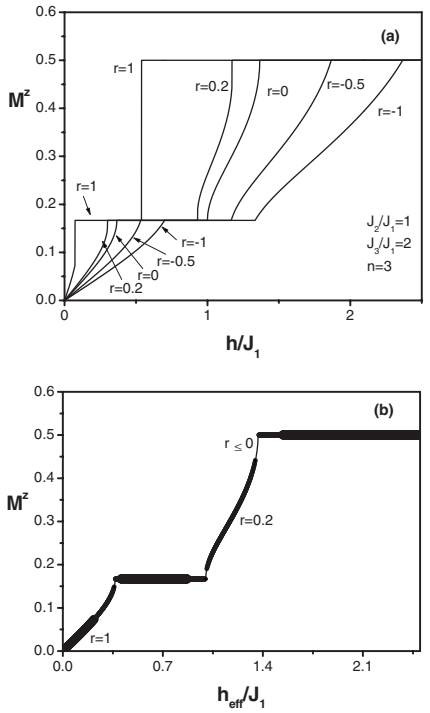

FIG. 5. (a) Magnetization as a function of h/J_1 and (b) universal curve for the magnetization as a function of the effective field h_{eff}/J_1 ($h_{\text{eff}}=h+2J'M^z$), at $T=0$, for different values of $r(r=J'/J_1)$, in the regions where the system undergoes first- ($r>0$) and second-order ($r\leq 0$) quantum transitions, for $n=3$ and $J_1=1$, $J_2=1$, and $J_3=2$.

press a phase transition. For $n=4$, this condition corresponds to $J_1J_3=J_2J_4$ and the phase diagram for this case is presented in Fig. 7. As it can be verified in this figure, we have three second-order lines, instead of four, and just one triple point.

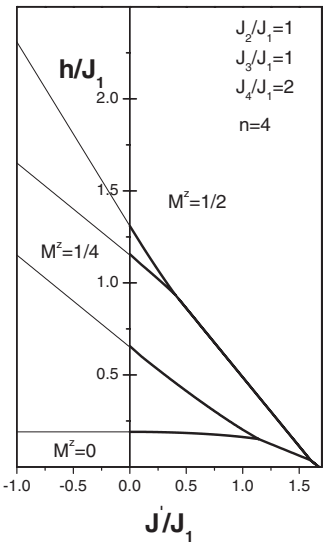

FIG. 6. Phase diagram for the quantum transitions as a function of the strength of the long-range interaction J'/J_1 for $n=4$ and $J_1=1$, $J_2=1$, $J_3=1$, and $J_4=2$. For $J'/J_1>0$, the critical lines identify the first-order phase transitions and for $J'/J_1\leq 0$, the second-order phase transitions.

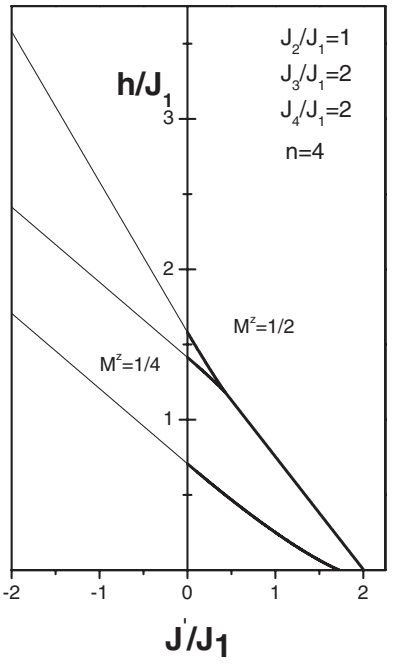

FIG. 7. Phase diagram for the quantum transitions as a function of the strength of the long-range interaction J'/J_1 for $n=4$ and $J_1=1$, $J_2=1$, $J_3=2$, and $J_4=2$. For $J'/J_1>0$, the critical lines identify the first-order phase transitions and for $J'/J_1\leq 0$, the second-order phase transitions.

The magnetization associated to the parameters defined in Fig. 6 is presented in Fig. 8. As in the previous cases, in Fig. 8(a) we have the magnetization as a function of the field for different values of J', and in Fig. 8(b), the universal curve

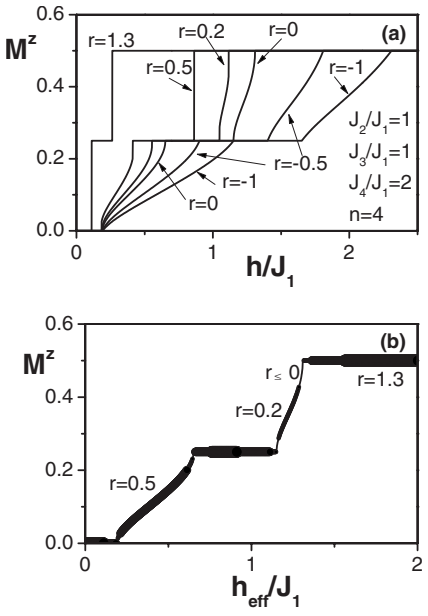

FIG. 8. (a) Magnetization as a function of h/J_1 and (b) universal curve for the magnetization as a function of the effective field h_{eff}/J_1 ($h_{\text{eff}}=h+2J'M^z$), at $T=0$, for different values of $r(r=J'/J_1)$, in the regions where the system undergoes first- ($r>0$) and second-order ($r\leq 0$) quantum transitions, for $n=4$ and $J_1=1$, $J_2=1$, $J_3=1$, and $J_4=2$.

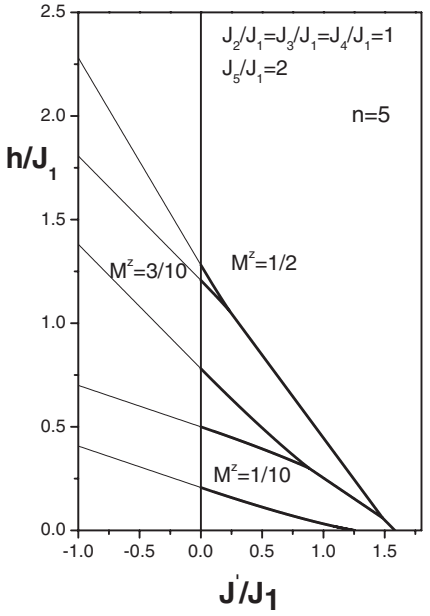

FIG. 9. Phase diagram for the quantum transitions as a function of the strength of the long-range interaction J'/J_1 for $n=5$ and $J_1=1$, $J_2=1$, $J_3=1$, $J_4=1$, and $J_5=2$. For $J'/J_1>0$, the critical lines identify the first-order phase transitions and for $J'/J_1\leq 0$, the second-order phase transitions.

for the magnetization as a function of the effective field h_{eff}. In Fig. 9, we present the phase diagram for $n=5$. Since n is odd, there is no suppression of any transition for $J'=0$ (Ref. 7) and, as expected, there are five second-order transition lines. The associated magnetization as a function of the field

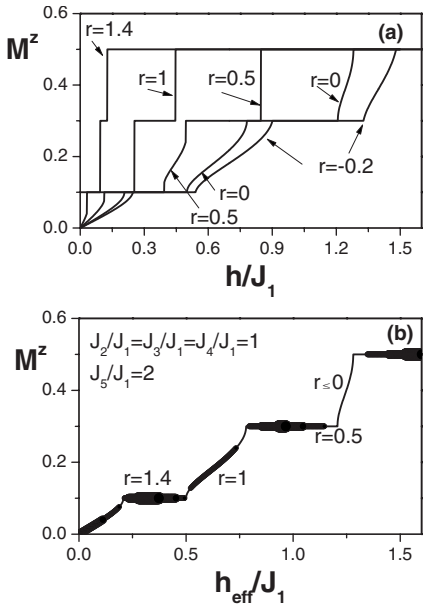

FIG. 10. (a) Magnetization as a function of h/J_1 and (b) universal curve for the magnetization as a function of the effective field h_{eff}/J_1 ($h_{\text{eff}}=h+2J'M^z$), at $T=0$, for different values of $r(r=J'/J_1)$, in the regions where the system undergoes first- ($r>0$) and second-order ($r\leq 0$) quantum transitions, for $n=5$ and $J_1=1$, $J_2=1$, $J_3=1$, $J_4=1$, and $J_5=2$.

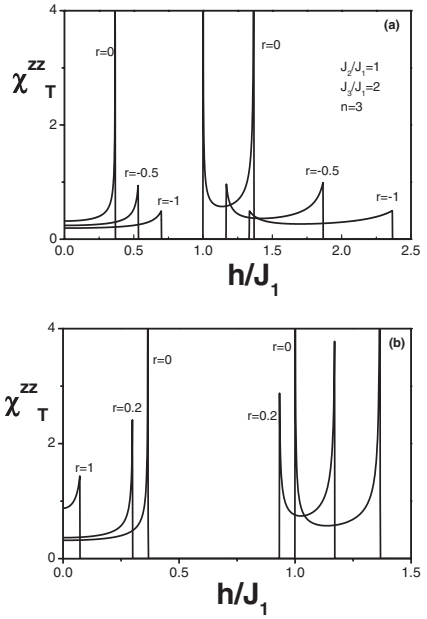

FIG. 11. Isothermal susceptibility χ_T^{zz}, at $T=0$, as a function of h/J_1, for $n=3$, $J_1=1$, $J_2=1$, $J_3=2$, and different values of $r(r=J'/J_1)$ (a) for $r\leq 0$ and (b) for $r\geq 0$.

is presented in Fig. 10(a) and the magnetization universal curve is shown in Fig. 10(b).

Finally, in Fig. 11, we present the isothermal susceptibility χ_T^{zz} for $n=3$ and different values of J'. As in the homogeneous model, the isothermal susceptibility, at the second-order phase transitions, diverges for $J'=0$ only, and its multiple phase transitions have the same critical exponents of the homogeneous model and consequently belong to the same universality class.

IV. CONCLUSIONS

In this work we have considered the isotropic *XY* model with a uniform long-range interaction along the z direction in a periodic inhomogenous lattice with N cells and n sites per cell. The exact solution of the model was formally obtained at arbitrary temperatures and distribution of magnetic moments and exchange constants. Explicit equations have been obtained for the functional of the Helmholtz free energy from which the equation of state can be determined numerically.

The analysis of the critical behavior has been restricted to the quantum phase transitions and we have shown, as in the homogeneous model, that the system presents first-order phase transitions when the long-range interaction is ferromagnetic and second-order phase transitions when the long-range interaction is antiferromagnetic. The model also presents multiple first- and second-order phase transitions and the number of critical lines is equal to n, for n odd, and less than n, for n even, provided the exchange constants in the xy plane satisfy a special relation.

The second-order critical lines meet the first-order ones at $J'=0$, which are bicritical points and there are multiple triple points, where three first-order critical lines meet, depending on the unit-cell size. The critical exponents have been ob-

tained numerically, and it has been shown, as expected, that the model belongs to the same universality class of the homogeneous one.

Finally, we would like to point out that is of paramount importance the presence of multiple first-order quantum transitions and triple points, which we have shown exactly to exist in the model, since we believe that this behavior is related to the different mechanisms from which the first-order phase transitions are driven. These mechanisms have been thoroughly discussed by Pfleiderer[16] by analyzing quantum critical behavior obtained for different materials.

ACKNOWLEDGMENTS

The authors would like to thank the Brazilian agencies CNPq and Capes for partial financial support.

*lindberg@fisica.ufc.br

[1] S. Sachdev, *Quantum Phase Transitions* (Cambridge University Press, Cambridge, England, 2000).
[2] P. Gambardella, A. Dallmeyer, K. Maiti, M. C. Malagoli, W. Eberhardt, K. Kern, and C. Carbone, Nature (London) **416**, 301 (2002).
[3] C. J. Mukherjee, R. Coldea, D. A. Tennant, M. Koza, M. Enderle, K. Habicht, P. Smeibidl, and Z. Tylczynski, J. Magn. Magn. Mater. **272-276**, 920 (2004).
[4] H. E. Lieb, T. Schultz, and D. C. Mattis, Ann. Phys. (N.Y.) **16**, 407 (1961).
[5] J. P. de Lima, L. L. Gonçalves, and T. F. A. Alves, Phys. Rev. B **75**, 214406 (2007).
[6] K. E. Feldman, J. Phys. A **39**, 1039 (2006).
[7] J. P. de Lima, T. F. A. Alves, and L. L. Gonçalves, J. Magn. Magn. Mater. **298**, 95 (2006).
[8] E. Dagotto and T. M. Rice, Science **271**, 618 (1996).
[9] T. N. Nguyen, P. A. Lee, and H. C. Loye, Science **271**, 489 (1996).
[10] M. Matsumoto, B. Normand, T. M. Rice, and M. Sigrist, Phys. Rev. B **69**, 054423 (2004).
[11] L. Amico, F. Baroni, A. Fubini, D. Patanè, V. Tognetti, and P. Verrucchi, Phys. Rev. A **74**, 022322 (2006).
[12] M. Avellino, A. J. Fisher, and S. Bose, Phys. Rev. A **74**, 012321 (2006).
[13] L. L. Gonçalves, A. P. Vieira, and L. P. S. Coutinho, J. Magn. Magn. Mater. **226-230**, 613 (2001).
[14] L. L. Gonçalves, L. P. S. Coutinho, and J. P. de Lima, Physica A **345**, 71 (2005).
[15] M. A. Continentino and A. S. Ferreira, Physica A **339**, 461 (2004).
[16] C. Pfleiderer, J. Phys.: Condens. Matter **17**, S987 (2005).
[17] Th. J. Siskens and P. Mazur, Physica (Amsterdam) **71**, 560 (1974).
[18] H. W. Capel and J. H. H. Perk, Physica A **87**, 211 (1977).
[19] L. L. Gonçalves, Ph.D. thesis, University of Oxford, 1977.
[20] F. F. Barbosa Filho, J. P. de Lima, and L. L. Gonçalves, J. Magn. Magn. Mater. **226-230**, 638 (2001).
[21] M. Oshikawa, M. Yamanaka, and I. Affleck, Phys. Rev. Lett. **78**, 1984 (1997).